



TECHNICAL DOCUMENT 3094
February 2000

**A Maximum-Likelihood-Based
Frequency Synchronizer for
Dual-H Full-Response 4-ARY
Continuous-Phase Modulation (CPM)**

R. H. Pettit
California State University, Northridge

B. E. Wahlen
SSC San Diego

Approved for public release;
distribution is unlimited.

SSC San Diego

20000302 084

TECHNICAL DOCUMENT 3094
February 2000

**A Maximum-Likelihood-Based
Frequency Synchronizer for
Dual-H Full-Response 4-ARY
Continuous-Phase Modulation (CPM)**

R. H. Pettit
California State University, Northridge

B. E. Wahlen
SSC San Diego

Approved for public release;
distribution is unlimited.



SSC San Diego
San Diego, CA 92152-5001

DTIC QUALITY INSPECTED 4

SSC SAN DIEGO
San Diego, California 92152-5001

E. L. Valdes, CAPT, USN
Commanding Officer

R. C. Kolb
Executive Director

ADMINISTRATIVE INFORMATION

The work described in this report was performed for the Office of Naval Research by the Signals Technology Branch D841, SSC San Diego.

Released by
B. L. Andersen, Head
Signals Technology Branch

Under authority of
D. O. Milstead, Head
RF Communications
Systems Division

A Maximum-Likelihood Based Frequency Synchronizer for Dual-h, Full Response 4-ary CPM

Ray H. Pettit and Bruce E. Wahlen

Abstract

Maximum-likelihood techniques are useful in finding synchronizer structures for various cases. Synchronizers for frequency, phase, and timing have been found for various bandpass signaling techniques such as PSK, DPSK, QAM, MSK, and CPM. These include data-aided, decision-directed, and clock-aided cases. For CPM, however, apparently only the single modulation index case has ML-based synchronizers.

This report describes a new non-data-aided, non-decision-directed ML-based frequency synchronizer (with no phase or timing information), derived for a full-response, dual-h (two modulation indexes), 4-ary CPM signaling scheme. The derived structure will be incorporated into future simulations to compare performance among several possible frequency synchronizers.

Keywords

Continuous-Phase Modulation, Frequency Synchronization, Maximum-Likelihood Estimation, Multi-h CPM, Digital Synchronizers

I. INTRODUCTION

Successful operation of digital communication systems requires that receivers achieve synchronization. Carrier frequency and phase, waveform time-of-arrival, frame synchronization for TDM/TDMA, and timing for a frequency-hopping pattern or for a direct sequence spreading code for spread-spectrum are examples of typical unknowns that must be estimated for good performance.

There are many successful synchronization schemes. Mengali and D'Andrea [1] present theoretical and practical details for various synchronizers for frequency, phase, and symbol timing. Their text deals with baseband and various bandpass signaling techniques, including PSK, DPSK, QAM, MSK, and CPM (single modulation index case). This paper concerns an important special version of CPM (Continuous Phase Modulation), namely dual-h, full-response with a rectangular frequency response function, and 4-ary signaling alphabet [2]. In addition to frequency, phase, and symbol timing, this case also requires the so-called "super-baud" synchronization inherent with CPM using several modulation indexes. The paper presents a structure for frequency acquisition and tracking for this case, based upon an optimum procedure known as "maximum likelihood" [3]. This is a standard criterion for optimality (maximization of a probability density function for received samples conditioned upon a set of parameters to be estimated). Future papers will address other levels of synchronization for this case.

Synchronizers often develop from good intuitive reasoning rather than from estimation theory. (In many cases, these ad hoc synchronizers fit within an estimation theory framework.) Others have been invented by adopting the techniques of estimation theory from the start. Both procedures are very useful. In this paper, the latter approach is followed. Even though the initial modeling and derivation efforts are for this "optimum" maximum-likelihood criterion, it should be emphasized that the inevitable necessary approximations for analytical completion and receiver implementation lead to sub-optimal final frequency recovery schemes. Final questions involving performance of this sub-optimal synchronizer will require simulation methods because of inherent analytical complexities. A direct measure of the "goodness" of an estimator is its variance, usually compared to either the Cramer-Rao or the Modified Cramer-Rao lower bounds (see [1], for example). Ultimately, desirable performance would be in terms of effects on ability to correctly receive data when using the particular synchronization method. A future paper will present results from appropriate simulation studies.

II. GENERAL STRUCTURE FOR THE FREQUENCY SYNCHRONIZER

The task at hand is to find a frequency recovery scheme (acquisition and tracking) that can operate without knowledge of the carrier's phase, symbol time-of-arrival, or data. That is, the synchronizer is to be non-data aided and non-decision directed. The notation and modeling closely follow Mengali and D'Andrea [1] as used for the single modulation index CPM considered in their text. Complex envelope notation is used for convenience. The paper's primary notation is given below.

We assume that the received waveform, $r(t)$, consists of the CPM signal and an additive white Gaussian noise component of spectral density, N_0 ,

$$r(t) = s(t) + w(t) \quad (1)$$

with

$$s(t) = e^{j(2\pi vt + \theta)} \sqrt{\frac{2E_s}{T}} e^{j\psi(t-\tau, \alpha)} \quad (2)$$

First author: Professor, Electrical and Computer Engineering Department, California State University, Northridge, CA 91330-8346. ray.pettit@csun.edu

Second author: Space and Naval Warfare Systems Center, San Diego, CA 92152 USA. wahlen@spawar.navy.mil

In (2), ν , θ , and τ represent the unknown parameters: frequency offset from the nominal carrier value, carrier phase, and time-of-arrival, respectively. E_s is the "energy" of the signal waveform over the symbol interval, T . The data sequence is $\alpha = (\dots, \alpha_{-1}, \alpha_0, \alpha_1, \dots)$, where $\alpha_i \in \{\pm 1, \pm 3\}$ for the 4-ary case of interest.

The phase $\psi(t, \alpha)$ is given by

$$\psi(t, \alpha) = 2\pi \sum_i \alpha_i h_i q(t - iT), \quad (3)$$

where h_i is the "modulation index" for the i^{th} interval. For our dual-h case, two modulation indexes are used, h_0 and h_1 , with h_0 associated with the even numbered intervals and h_1 with the odd ones. Thus,

$$\begin{aligned} \psi(t, \alpha) &= \psi_1(t, \alpha_e) + \psi_2(t, \alpha_o) \\ &= 2\pi \left\{ h_0 \sum_i \alpha_{2i} q(t - 2iT) + h_1 \sum_i \alpha_{2i+1} q(t - [2i+1]T) \right\}. \end{aligned} \quad (4)$$

In (3), $q(t)$ is the phase response function, which is shown below for the full-response rectangular-frequency-pulse case (so-called 1 REC):

$$q(t) = \begin{cases} 0, & \text{if } t < 0 \\ \frac{t}{2T}, & \text{if } 0 \leq t \leq T \\ \frac{1}{2}, & \text{if } t > T. \end{cases} \quad (5)$$

In keeping with modern practice, processing of discrete-time samples will be performed by the synchronizer, a so-called "digital synchronizer," instead of an "analog synchronizer" that processes directly the continuous-time waveforms. See figure 1. The samples $\mathbf{x} = \{x(kT_s)\}$ are taken from the output of an "anti-aliasing" filter, AAF, which is assumed to have sufficiently wide passband to pass through the signal, $s(t)$, without significant distortion. The sampling period, T_s , is sufficiently short to allow the samples to retain the information content of the continuous-time waveforms.

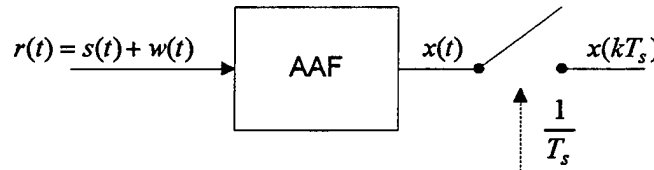


Fig. 1. Sampling output of anti-aliasing filter.

For some additional notation, we let L_0 be the number of information symbols to be "observed" for purposes of collecting the samples, and let N be the number of samples taken for each symbol. (Mengali and D'Andrea suggest $N = 4$ as an appropriate value for cases studied by them.) Thus,

$$\begin{aligned} T_0 &= \text{"observation time"} \\ &= L_0 T \\ &= NL_0 T_s \end{aligned} \quad (6)$$

and

$$\mathbf{x} = \{x(0), x(T_s), \dots, x([NL_0 - 1]T_s)\}. \quad (7)$$

Since the task is to derive a maximum-likelihood based estimator of the unknown frequency offset, ν , which does not require knowledge of $\{\theta, \tau, \alpha\}$, we require the "Likelihood Function," $\Lambda(\mathbf{x}|\tilde{\nu})$, which will be obtained from the "Conditional Likelihood Function," $\Lambda(\mathbf{x}|\tilde{\alpha}, \tilde{\nu}, \tilde{\theta}, \tilde{\tau})$, by averaging over $\{\tilde{\alpha}, \tilde{\theta}, \tilde{\tau}\}$. (See, for example, Van Trees [3] for an excellent treatment of detection and estimation theory.)

Before continuing, some clarification of notation is in order. For example,

$$\begin{aligned} \nu &= \text{actual, but unknown, frequency offset} \\ \tilde{\nu} &= \text{a possible value of } \nu \text{ (a "realization")} \\ \hat{\nu} &= \text{an estimate of } \nu. \end{aligned}$$

The conditional likelihood function is given by

$$\Lambda(\mathbf{x}|\tilde{\alpha}, \tilde{\nu}, \tilde{\theta}, \tilde{\tau}) = \exp \left\{ \frac{T_s}{N_0} \operatorname{Re} \left[\sum_{k=0}^{NL_0-1} x(kT_s) \tilde{s}^*(kT_s) \right] - \frac{T_s}{2N_0} \sum_{k=0}^{NL_0-1} |\tilde{s}(kT_s)|^2 \right\} \quad (8)$$

with

$$\tilde{s}(t) = e^{j(2\pi\tilde{v}t + \tilde{\theta})} \sqrt{\frac{2E_s}{T}} e^{j\psi_1(t-\tilde{\tau}, \tilde{\alpha}_e)} e^{j\psi_2(t-\tilde{\tau}, \tilde{\alpha}_o)}. \quad (9)$$

Since the last sum in (8) is independent of $\{\tilde{\alpha}, \tilde{v}, \tilde{\theta}, \tilde{\tau}\}$, it is sufficient to consider

$$\begin{aligned} \Lambda'(\mathbf{x}|\tilde{\alpha}, \tilde{v}, \tilde{\theta}, \tilde{\tau}) &= \exp \left\{ \frac{T_s}{N_0} \operatorname{Re} \left[\sum_{k=0}^{NL_0-1} \mathbf{x}(kT_s) \tilde{s}^*(kT_s) \right] \right\} \\ &= \exp \left\{ \frac{T_s}{N_0} \sqrt{\frac{2E_s}{T}} \operatorname{Re} \left[e^{-j\tilde{\theta}} \sum_{k=0}^{NL_0-1} \mathbf{x}(kT_s) e^{-j2\pi\tilde{v}kT_s} \right. \right. \\ &\quad \left. \left. \cdot e^{-j\psi_1(kT_s-\tilde{\tau}, \tilde{\alpha}_e)} e^{-j\psi_2(kT_s-\tilde{\tau}, \tilde{\alpha}_o)} \right] \right\}. \end{aligned} \quad (10)$$

By definition, the "maximum likelihood estimate of v " is the value of \tilde{v} that maximizes $\Lambda(\mathbf{x}|\tilde{v})$.

To proceed, we define

$$X \equiv \sum_{k=0}^{NL_0-1} \mathbf{x}(kT_s) e^{-j2\pi\tilde{v}kT_s} e^{-j\psi_1(kT_s-\tilde{\tau}, \tilde{\alpha}_e)} e^{-j\psi_2(kT_s-\tilde{\tau}, \tilde{\alpha}_o)} \quad (11)$$

(the magnitude of the complex X is $|X|$ and its angle is ϕ_X ; i.e., $X = |X| e^{j\phi_X}$). Noting that X is independent of $\tilde{\theta}$, we have

$$\Lambda'(\mathbf{x}|\tilde{\alpha}, \tilde{v}, \tilde{\theta}, \tilde{\tau}) = \exp \left\{ C |X| \cos(\phi_X - \tilde{\theta}) \right\} \quad (12)$$

with

$$C = \frac{T_s}{N_0} \sqrt{\frac{2E_s}{T}}.$$

First we average over $\tilde{\theta}$, assuming that $\tilde{\theta}$ is uniform $(0, 2\pi)$:

$$\begin{aligned} \Lambda'(\mathbf{x}|\tilde{\alpha}, \tilde{v}, \tilde{\tau}) &= \frac{1}{2\pi} \int_0^{2\pi} \exp \left\{ C |X| \cos(\phi_X - \tilde{\theta}) d\tilde{\theta} \right\} \\ &= I_0(C|X|). \end{aligned} \quad (13)$$

$I_0(\cdot)$ is the zeroth order, modified Bessel Function of the First Kind, a real monotonically increasing function of its argument.

It is not analytically feasible to obtain the exact \hat{v}_{ML} at this point, so we proceed based on the special case of low signal-to-noise ratio. This allows the approximation,

$$I_0(C|X|) \cong 1 + \frac{C^2}{4} |X|^2, \quad (14)$$

and leads ultimately to a maximum-likelihood based estimator of v . Maximizing $\Lambda'(\mathbf{x}|\tilde{v})$ is therefore approximately equivalent to maximizing

$$\Lambda''(\mathbf{x}|\tilde{v}) \equiv E_{\tilde{\alpha}, \tilde{\tau}} \left\{ |X|^2 \right\}, \quad (15)$$

where (15) implies averaging $|X|^2$ over $(\tilde{\alpha}, \tilde{\tau})$. Appendix A presents the details of this averaging, showing that

$$\Lambda''(\mathbf{x}|\tilde{v}) = \sum_{k_1=0}^{NL_0-1} \sum_{k_2=0}^{NL_0-1} \mathbf{x}(k_1T_s) \mathbf{x}^*(k_2T_s) e^{-j[2\pi(k_1-k_2)\tilde{v}T_s]} H[k_1T_s, k_2T_s], \quad (16)$$

where $H[k_1T_s, k_2T_s]$ is defined by

$$\begin{aligned} H[k_1T_s, k_2T_s] &\equiv \frac{1}{2T} \int_0^{2T} \prod_{i=-\infty}^{\infty} \left[\frac{1 \sin(8\pi h_0 p [k_2T_s - \tilde{\tau} - 2iT, (k_2 - k_1)T_s])}{4 \sin(2\pi h_0 p [k_2T_s - \tilde{\tau} - 2iT, (k_2 - k_1)T_s])} \right. \\ &\quad \left. \cdot \frac{1 \sin(8\pi h_1 p [k_2T_s - \tilde{\tau} - (2i+1)T, (k_2 - k_1)T_s])}{4 \sin(2\pi h_1 p [k_2T_s - \tilde{\tau} - (2i+1)T, (k_2 - k_1)T_s])} \right] d\tilde{\tau}. \end{aligned} \quad (17)$$

In (17), $p(t, \Delta t)$ is defined by

$$p(t, \Delta t) \equiv q(t) - q(t - \Delta t). \quad (18)$$

By changing the variable of integration in (17) to $t = k_2 T_s - \tilde{\tau}$ and noting that the integrand is periodic with period $2T$, we have

$$\begin{aligned} H[k_1 T_s, k_2 T_s] &\equiv H[(k_2 - k_1) T_s] = H[(k_1 - k_2) T_s] \\ &= \frac{1}{2T} \int_0^{2T} \prod_{i=-\infty}^{\infty} \left[\frac{1 \sin(8\pi h_0 p [t - 2iT, (k_2 - k_1) T_s])}{4 \sin(2\pi h_0 p [t - 2iT, (k_2 - k_1) T_s])} \right. \\ &\quad \left. \cdot \frac{1 \sin(8\pi h_1 p [t - (2i+1)T, (k_2 - k_1) T_s])}{4 \sin(2\pi h_1 p [t - (2i+1)T, (k_2 - k_1) T_s])} \right] dt. \end{aligned} \quad (19)$$

The general structure for the frequency synchronizer can now be developed, paralleling Mengali and D'Andrea's development for the single-h case [1], although significant additional work must be carried out to produce a synchronizer of reasonable implementation complexity. Section III will describe the additional work.

We seek the value of \tilde{v} that maximizes $\Lambda''(\mathbf{x}|\tilde{v})$, as shown in (16). We take the derivative and set the result to zero, in the usual way:

$$\begin{aligned} \frac{d\Lambda''(\mathbf{x}|\tilde{v})}{d\tilde{v}} &= j2\pi T_s \sum_{k_1=0}^{NL_0-1} \sum_{k_2=0}^{NL_0-1} \left[x(k_1 T_s) e^{-j2\pi k_1 T_s \tilde{v}} \right. \\ &\quad \left. \cdot x^*(k_2 T_s) e^{+j2\pi k_2 T_s \tilde{v}} (k_2 - k_1) H[(k_2 - k_1) T_s] \right] \\ &= 0. \end{aligned} \quad (20)$$

Because $\Lambda''(\mathbf{x}|\tilde{v})$ is real, so is its derivative, and thus the term in (20) represented by the double summation is imaginary. Now define

$$\begin{aligned} y(k T_s) &\equiv x(k T_s) e^{-j2\pi k \tilde{v} T_s} \\ h(k T_s) &\equiv (k - k_1) H[(k - k_1) T_s]. \end{aligned} \quad (21)$$

We seek the value of \tilde{v} to satisfy

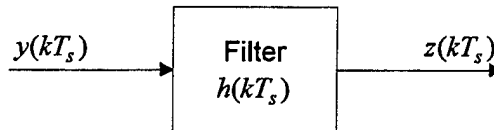
$$\text{Im} \left\{ \sum_{k_1=0}^{NL_0-1} y(k_1 T_s) \left[\sum_{k_2=0}^{NL_0-1} y(k_2 T_s) h[(k_1 - k_2) T_s] \right]^* \right\} = 0. \quad (22)$$

Let

$$\begin{aligned} z(k T_s) &= \sum_{k_2=0}^{NL_0-1} y(k_2 T_s) h[(k - k_2) T_s] \\ &= y(k T_s) * h(k T_s). \end{aligned} \quad (23)$$

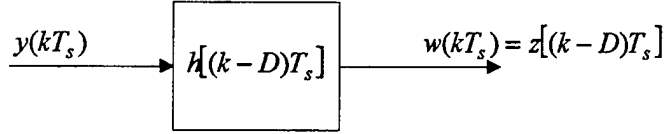
(Since $h(k T_s)$ is real, $z^*(k T_s) = \sum_{k_2=0}^{NL_0-1} y^*(k_2 T_s) h[(k - k_2) T_s]$).

Thus, $h(k T_s)$ can be interpreted as a digital filter's impulse response and $z(k T_s)$ as its output with $y(k T_s)$ being the input.



Before proceeding to the final general structure, we recognize that $h(k T_s)$ is non-causal. This requires that a suitable delay of D sampling intervals be incorporated into $h(k T_s)$ to have physical realizability. Mengali and D'Andrea [1] for a similar situation state that $D = 2N$ is probably adequate, but further study of this point will be needed for our case and will be part of the associated simulation studies. In Section III we will provide considerably more detail about $h(k T_s)$, thus providing the basis for the final simulation steps.

We show the delay, D , as follows:



Now we re-write (22) as follows:

$$\sum_{k_1=D}^{NL_0-1+D} \text{Im} \{y[(k-D)T_s] w^*(kT_s)\} = 0. \quad (24)$$

Equation (24) provides the basis for the general structure. The basic idea is to exploit the sum of some consecutive terms in the above, say, N terms, as an error signal to drive $\frac{d\hat{v}}{dv}(\hat{v})$ towards zero.

The frequency estimates are to be updated according to

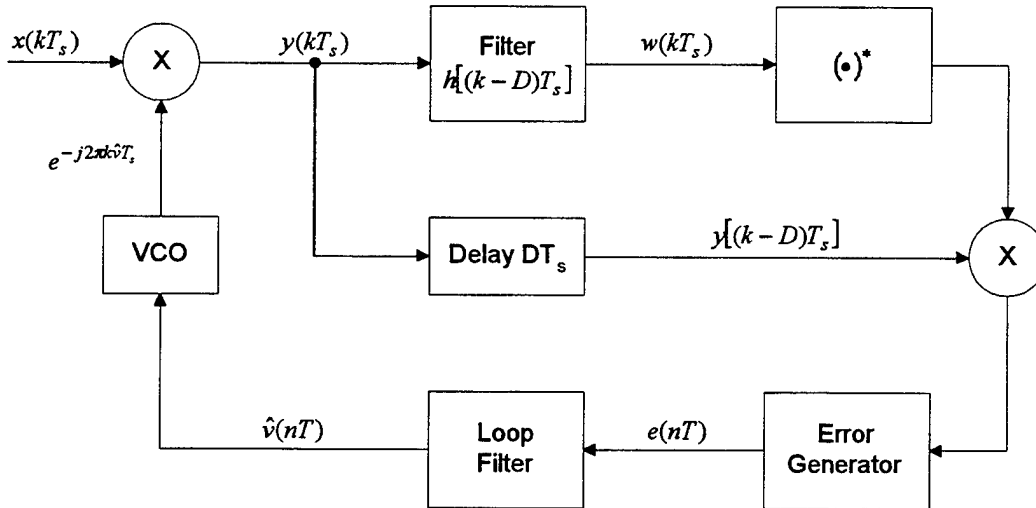
$$\hat{v}[(n+1)T] = \hat{v}[nT] + \gamma e[nT], \quad (25)$$

where γ is a step-size parameter and $e[nT]$ is the error signal,

$$e[nT] = \sum_{k=nN}^{(n+1)N-1} \text{Im} \{y(kT_s) w^*(kT_s)\}. \quad (26)$$

The result is the structure shown in Figure 2. (In (26), n is the symbol index and k is the sample index).

The approach described above is a standard one for finding synchronizer structures with closed-loop feedback processing. (See [1].) The parameter, γ , selected based on simulation studies, should not be so large as to cause large variations of the estimate about the true value nor so small as to require excessive time to converge to the true value.



$$\hat{v}[(n+1)T] = \hat{v}(nT) + \gamma e(nT)$$

Fig. 2. General structure for frequency synchronizer

The general structure shown in Figure 2 is identical to Figure 4.10 of [1] for the single-h CPM case. The effects of dual-h CPM are incorporated in the details of $h(kT_s)$, which seem to be significantly different from the $h(kT_s)$ of single-h CPM in [1]. Section III will now derive and discuss these additional details.

III. THE FEEDFORWARD FILTER, $h(kT_s)$

The function, $p(t, kT_s)$ (and all versions of it shifted by integer multiples of NT_s), holds the key to understanding $H[(k_2 - k_1)T_s]$, shown in (19), and to implementing $h(kT_s) = kH[kT_s]$. Because $p(t, kT_s)$ has finite width (see Appendix B for details of $p(t, kT_s)$ as a function of $k = k_2 - k_1$), there are only a finite number of factors in the product of (19)

that differ from unity. That is, if both $p[t - 2iT, kT_s]$ and $p[t - (2i + 1)T, kT_s]$ are zero over the range of the integral, $(0, 2T)$ (for a particular value of k), that particular i th factor equals unity. Therefore, the only values of i in the product of (19) that are significant to the understanding of the behavior of $H(kT_s)$ are those for which the corresponding factors differ from unity.

In Appendix C, these "significant" values for i are shown as follows:

k	Set of Significant Values of i (from Equation (19))
$0 < k \leq N$	0, -1
$k > N$	$0, -1, \dots, -\left[\frac{k}{2N}\right]_{\text{int}}^+$
$-N \leq k < 0$	0, 1
$k < -N$	$0, 1, \dots, \left[-\frac{k}{2N}\right]_{\text{int}}^+$

In the above, $\left[\frac{k}{2N}\right]_{\text{int}}^+$ represents the next integer equal to or exceeding $\frac{k}{2N}$.

Using the above, $\Lambda''(\mathbf{x}|\tilde{v})$ from (16) can be re-written as follows, requiring only a finite number of factors to be considered:

$$\Lambda''(\mathbf{x}|\tilde{v}) = \sum_{k_1=0}^{NL_0-1} x(k_1T_s) e^{-j2\pi k_1 \tilde{v} T_s} G(k_1, k_2, \tilde{v}), \quad (27)$$

where

$$\begin{aligned} G(k_1, k_2, \tilde{v}) = & \sum_{k_2=0}^{k_1-N-1} x^*(k_2T_s) e^{j2\pi k_2 \tilde{v} T_s} \frac{1}{2T} \int_0^{2T} \prod_{i=0}^{\left[\frac{k_1-k_2}{2N}\right]_{\text{int}}^+} (\cdot) dt \\ & + \sum_{k_2=k_1-N}^{k_1-1} x^*(k_2T_s) e^{j2\pi k_2 \tilde{v} T_s} \frac{1}{2T} \int_0^{2T} \prod_{i=0}^1 (\cdot) dt \\ & + \sum_{k_2=k_1+1}^{N+k_1} x^*(k_2T_s) e^{j2\pi k_2 \tilde{v} T_s} \frac{1}{2T} \int_0^{2T} \prod_{i=-1}^0 (\cdot) dt \\ & + \sum_{k_2=N+k_1+1}^{NL_0-1} x^*(k_2T_s) e^{j2\pi k_2 \tilde{v} T_s} \frac{1}{2T} \int_0^{2T} \prod_{i=-\left[\frac{k_2-k_1}{2N}\right]_{\text{int}}^+}^0 (\cdot) dt \end{aligned} \quad (28)$$

and

$$\begin{aligned} (\cdot) = & \frac{1 \sin(8\pi h_0 p [t - 2iT, (k_2 - k_1)T_s])}{4 \sin(2\pi h_0 p [t - 2iT, (k_2 - k_1)T_s])} \\ & \frac{1 \sin(8\pi h_1 p [t - (2i + 1)T, (k_2 - k_1)T_s])}{4 \sin(2\pi h_1 p [t - (2i + 1)T, (k_2 - k_1)T_s])}. \end{aligned} \quad (29)$$

(See (19)).

The next step for understanding and implementing $h(kT_s)$ is the evaluation of the four integrals of (28). Many tedious steps are required. From Appendix D, we have the following results:

Case 1: $0 \leq k_2 \leq k_1 - N - 1$

$$\begin{aligned} F_1(k_1T_s, k_2T_s) & \equiv \frac{1}{2T} \int_0^{2T} \prod_{i=0}^{\left[\frac{k_1-k_2}{2N}\right]_{\text{int}}^+} (\cdot) dt \\ & \cong [\cos \pi h_0 \cos \pi h_1 \cos 2\pi h_0 \cos 2\pi h_1]^{1 + \left[\frac{k_1-k_2}{2N}\right]_{\text{int}}^+} \\ & = F_1 [(k_2 - k_1)T_s] \end{aligned} \quad (30)$$

Case 2: $k_1 - N \leq k_2 \leq k_1 - 1$

$$\begin{aligned}
F_2(k_1 T_s, k_2 T_s) &\equiv \frac{1}{2T} \int_0^{2T} \prod_{i=0}^1 (\cdot) dt & (31) \\
&= \frac{1}{4} \left[1 + \frac{(k_2 - k_1)}{N} \right] \left[\cos \frac{3\pi h_0 (k_2 - k_1)}{N} + \cos \frac{\pi h_0 (k_2 - k_1)}{N} \right. \\
&\quad \left. + \cos \frac{3\pi h_1 (k_2 - k_1)}{N} + \cos \frac{\pi h_1 (k_2 - k_1)}{N} \right] \\
&\quad + \frac{1}{4\pi} \left\{ \left[\frac{h_1}{3(h_0^2 - h_1^2)} + \frac{3h_1}{h_0^2 - 9h_1^2} \right] \sin \frac{3\pi h_1 (k_2 - k_1)}{N} \right. \\
&\quad + \left[\frac{h_1}{9h_0^2 - h_1^2} + \frac{h_1}{h_0^2 - h_1^2} \right] \sin \frac{\pi h_1 (k_2 - k_1)}{N} \\
&\quad + \left[\frac{h_0}{9h_1^2 - h_0^2} + \frac{h_0}{h_1^2 - h_0^2} \right] \sin \frac{\pi h_0 (k_2 - k_1)}{N} \\
&\quad \left. + \left[\frac{h_0}{3(h_1^2 - h_0^2)} + \frac{3h_0}{h_1^2 - 9h_0^2} \right] \sin \frac{3\pi h_0 (k_2 - k_1)}{N} \right\} \\
&= F_2 [(k_2 - k_1) T_s]
\end{aligned}$$

Case 3: $k_1 + 1 \leq k_2 \leq N + k_1$

$$\begin{aligned}
F_3(k_1 T_s, k_2 T_s) &\equiv \frac{1}{2T} \int_0^{2T} \prod_{i=-1}^0 (\cdot) dt & (32) \\
&= \frac{1}{4} \left[1 - \frac{(k_2 - k_1)}{N} \right] \left[\cos \frac{3\pi h_0 (k_2 - k_1)}{N} + \cos \frac{\pi h_0 (k_2 - k_1)}{N} \right. \\
&\quad \left. + \cos \frac{3\pi h_1 (k_2 - k_1)}{N} + \cos \frac{\pi h_1 (k_2 - k_1)}{N} \right] \\
&\quad + \frac{1}{4\pi} \left\{ \left[\frac{h_1}{3(h_1^2 - h_0^2)} + \frac{3h_1}{9h_1^2 - h_0^2} \right] \sin \frac{3\pi h_1 (k_2 - k_1)}{N} \right. \\
&\quad + \left[\frac{h_1}{h_1^2 - 9h_0^2} + \frac{h_1}{h_1^2 - h_0^2} \right] \sin \frac{\pi h_1 (k_2 - k_1)}{N} \\
&\quad + \left[\frac{h_0}{h_0^2 - 9h_1^2} + \frac{h_0}{h_0^2 - h_1^2} \right] \sin \frac{\pi h_0 (k_2 - k_1)}{N} \\
&\quad \left. + \left[\frac{h_0}{3(h_0^2 - h_1^2)} + \frac{3h_0}{9h_0^2 - h_1^2} \right] \sin \frac{3\pi h_0 (k_2 - k_1)}{N} \right\} \\
&= F_3 [(k_2 - k_1) T_s]
\end{aligned}$$

Case 4: $N + k_1 + 1 \leq k_2 \leq NL_0 - 1$

$$\begin{aligned}
F_4(k_1 T_s, k_2 T_s) &\equiv \frac{1}{2T} \int_0^{2T} \prod_{i=-\left[\frac{k_2 - k_1}{2N}\right]_{int}^+}^0 (\cdot) dt & (33) \\
&\cong [\cos \pi h_0 \cos \pi h_1 \cos 2\pi h_0 \cos 2\pi h_1]^{1+\left[\frac{k_2 - k_1}{2N}\right]_{int}^+} \\
&= F_4 [(k_2 - k_1) T_s]
\end{aligned}$$

As discussed in Appendix D, analytical complexities led to the need for the approximations used to obtain $F_1 [(k_2 - k_1) T_s]$ and $F_4 [(k_2 - k_1) T_s]$. Exact results were obtained for $F_2 [(k_2 - k_1) T_s]$ and $F_3 [(k_2 - k_1) T_s]$.

It appears that $F_1 [(k_2 - k_1) T_s]$ and $F_4 [(k_2 - k_1) T_s]$ make only small contributions to $G(k_1, k_2, \tilde{v})$ in (28) and, therefore, they will be discarded for the sequel. This allows for a simple implementation of $h(k T_s)$ and provides for a reasonable delay, D . Note that $F_2 [(k_2 - k_1) T_s]$ and $F_3 [(k_2 - k_1) T_s]$ are easily calculated for fixed values of h_0 and h_1 .

The digital filter, $h(kT_s)$, in Figure 2 can now be more specifically given by

$$\begin{aligned} h(kT_s) &= kH(kT_s) \\ &= kF_2(kT_s), \text{ for } -N \leq k \leq -1 \\ &= kF_3(kT_s), \text{ for } 1 \leq k \leq N \\ &= 0, \text{ for } k = 0 \text{ and } |k| > N. \end{aligned}$$

(See Equations (31), (32) for $F_2(kT_s)$, $F_3(kT_s)$, respectively). Note that $H[kT_s]$ is an even function of k and, therefore, $h(kT_s)$ is odd.

IV. SUMMARY AND CONCLUSIONS

This paper presents the derivation of a frequency synchronizer for dual-h, full-response, 4-ary CPM (rectangular frequency response function). The synchronizer is based upon the Maximum-Likelihood criterion, with the final structure resulting from certain approximations made to overcome various mathematical complexities and to make any subsequent implementation of reasonable complexity.

It is not clear that this new synchronizer provides significant, if any, benefits compared with others in use or proposed for specific applications. Comparisons based upon simulation are required before any further conclusions can be drawn.

REFERENCES

- [1] U. Mengali and A. N. D'Andrea, *Synchronization Techniques for Digital Receivers*, New York:Plenum Press, 1997.
- [2] J. B. Anderson, T. Aulin, and C-E. Sundberg, *Digital Phase Modulation*, New York:Plenum Press, 1986.
- [3] H. L. Van Trees, *Detection, Estimation, and Modulation: Part I*, New York:Wiley, 1968.

APPENDIX A: Derivation of $\Lambda''(\mathbf{x}|\tilde{v})$

Since $\Lambda''(\mathbf{x}|\tilde{v}) \equiv E_{\tilde{\alpha}_e, \tilde{\tau}} \{ |X|^2 \}$, we begin with (using (11))

$$\begin{aligned} |X|^2 &\equiv \sum_{k_1=0}^{NL_0-1} \sum_{k_2=0}^{NL_0-1} x(k_1T_s) x^*(k_2T_s) e^{-j2\pi(k_1-k_2)\tilde{v}T_s} \\ &\quad \cdot e^{-j\psi_1(k_1T_s-\tilde{\tau}, \tilde{\alpha}_e)} e^{+j\psi_1(k_2T_s-\tilde{\tau}, \tilde{\alpha}_e)} \\ &\quad \cdot e^{-j\psi_2(k_1T_s-\tilde{\tau}, \tilde{\alpha}_o)} e^{+j\psi_2(k_2T_s-\tilde{\tau}, \tilde{\alpha}_o)}. \end{aligned} \quad (\text{A1})$$

Because the data symbols are independent, the averaging over α can be separated into the $\tilde{\alpha}_e$ and $\tilde{\alpha}_o$ terms. Consider the first term,

$$\begin{aligned} &E_{\tilde{\alpha}_e} \left\{ e^{-j\psi_1(k_1T_s-\tilde{\tau}, \tilde{\alpha}_e)} e^{+j\psi_1(k_2T_s-\tilde{\tau}, \tilde{\alpha}_e)} \right\} \\ &= E_{\tilde{\alpha}_e} \left\{ e^{-j2\pi h_0 \left(\sum_i \tilde{\alpha}_{2i} [q(k_1T_s-\tilde{\tau}-2iT)-q(k_2T_s-\tilde{\tau}-2iT)] \right)} \right\} \\ &= \prod_i E_{\tilde{\alpha}_{2i}} \left\{ e^{j2\pi h_0 \tilde{\alpha}_{2i} [q(k_2T_s-\tilde{\tau}-2iT)-q(k_1T_s-\tilde{\tau}-2iT)]} \right\}. \end{aligned} \quad (\text{A2})$$

The last step follows because the $\tilde{\alpha}_{2i}$ are independent.

By defining

$$p(t, \Delta t) \equiv q(t) - q(t - \Delta t), \quad (\text{A3})$$

the above product can be rewritten as

$$\prod_i E_{\tilde{\alpha}_{2i}} \left\{ e^{j2\pi h_0 \tilde{\alpha}_{2i} p[k_2T_s-\tilde{\tau}-2iT, (k_2-k_1)T_s]} \right\}. \quad (\text{A4})$$

Now, we consider each factor separately.

$$\begin{aligned} &E_{\tilde{\alpha}_{2i}} \left\{ e^{j2\pi h_0 \tilde{\alpha}_{2i} p[k_2T_s-\tilde{\tau}-2iT, (k_2-k_1)T_s]} \right\} \\ &= \frac{1}{4} \left\{ e^{j6\pi h_0 p[k_2T_s-\tilde{\tau}-2iT, (k_2-k_1)T_s]} \right. \\ &\quad + e^{j2\pi h_0 p[k_2T_s-\tilde{\tau}-2iT, (k_2-k_1)T_s]} \\ &\quad + e^{-j2\pi h_0 p[k_2T_s-\tilde{\tau}-2iT, (k_2-k_1)T_s]} \\ &\quad \left. + e^{-j6\pi h_0 p[k_2T_s-\tilde{\tau}-2iT, (k_2-k_1)T_s]} \right\}, \end{aligned} \quad (\text{A5})$$

which is of the form,

$$\begin{aligned}
 \frac{1}{4} (e^{j3\beta} + e^{j\beta} + e^{-j\beta} + e^{-j3\beta}) &= \frac{1}{2} (\cos 3\beta + \cos \beta) \\
 &= \cos \beta \cos 2\beta \\
 &= \frac{1}{2} \frac{\sin 2\beta \cos 2\beta}{\sin \beta} \\
 &= \frac{1}{4} \frac{\sin 4\beta}{\sin \beta}.
 \end{aligned} \tag{A6}$$

Thus,

$$\begin{aligned}
 &E_{\tilde{\alpha}_{2i}} \left\{ e^{j2\pi h_0 \tilde{\alpha}_{2i} p [k_2 T_s - \tilde{\tau} - 2iT, (k_2 - k_1)T_s]} \right\} \\
 &= \frac{1 \sin (8\pi h_0 p [k_2 T_s - \tilde{\tau} - 2iT, (k_2 - k_1)T_s])}{4 \sin (2\pi h_0 p [k_2 T_s - \tilde{\tau} - 2iT, (k_2 - k_1)T_s])}.
 \end{aligned} \tag{A7}$$

Similarly,

$$\begin{aligned}
 &E_{\tilde{\alpha}_{2i+1}} \left\{ e^{j2\pi h_1 \tilde{\alpha}_{2i+1} p [k_2 T_s - \tilde{\tau} - (2i+1)T, (k_2 - k_1)T_s]} \right\} \\
 &= \frac{1 \sin (8\pi h_1 p [k_2 T_s - \tilde{\tau} - (2i+1)T, (k_2 - k_1)T_s])}{4 \sin (2\pi h_1 p [k_2 T_s - \tilde{\tau} - (2i+1)T, (k_2 - k_1)T_s])}.
 \end{aligned} \tag{A8}$$

Using (A7) and (A8), and then averaging over the uniform $\tilde{\tau}$, $(0, 2T)$, gives (17).

APPENDIX B: The Function $p[t, kT_s]$

The function, $p[t, kT_s] = q(t) - q(t - kT_s)$, is a function of k and is shown below for reference.

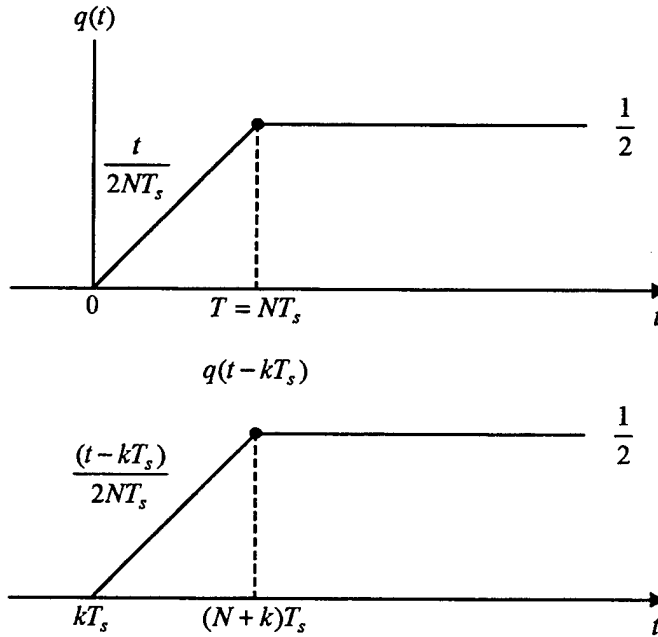
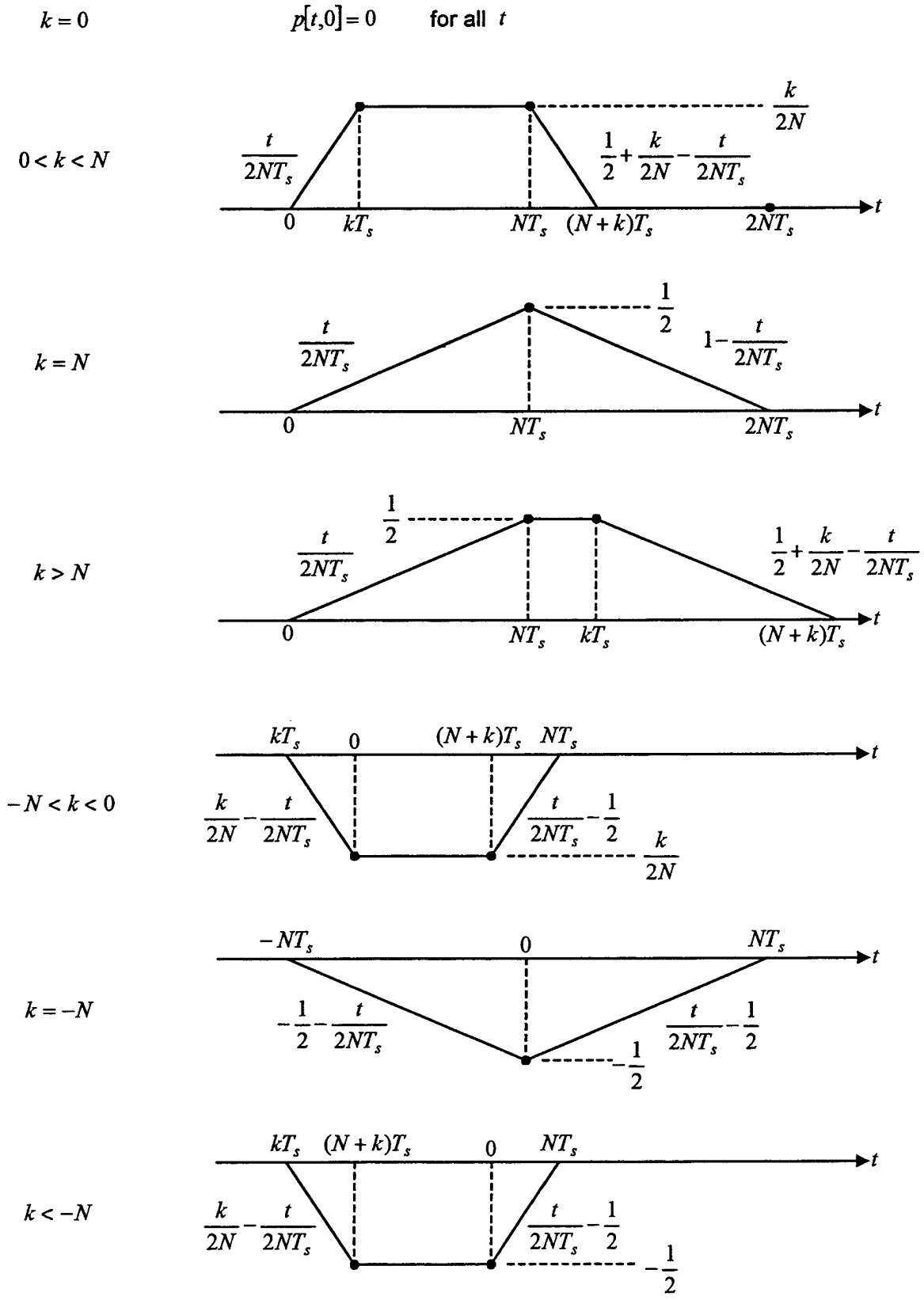


Table of $p[t, kT_s]$

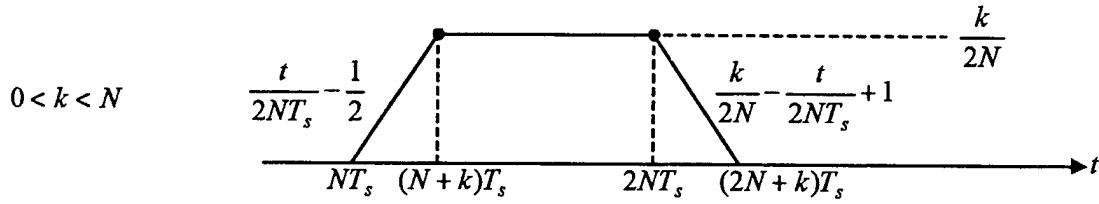


(note: not drawn to scale)

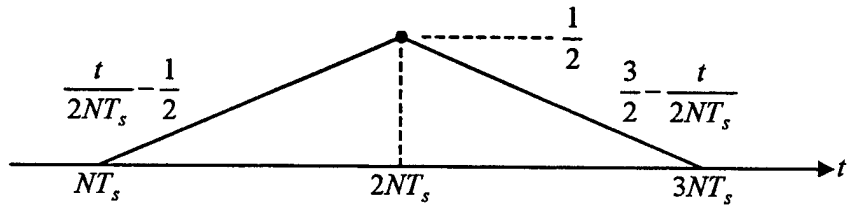
Table of $p[t-T, kT_s] = p[t-NT_s, kT_s]$

$k = 0$

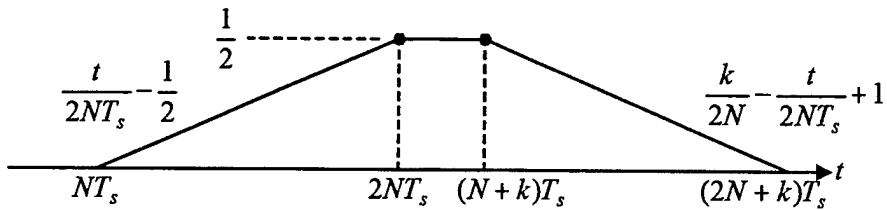
$p[t-NT_s, 0] = 0$ for all t



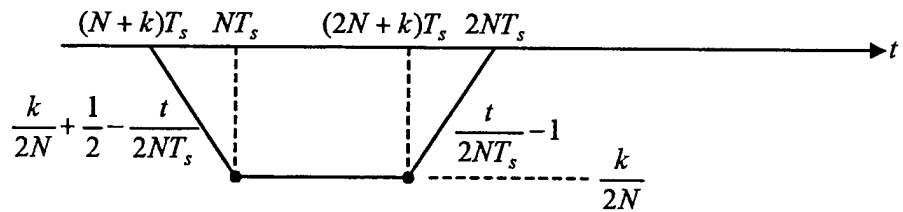
$k = N$



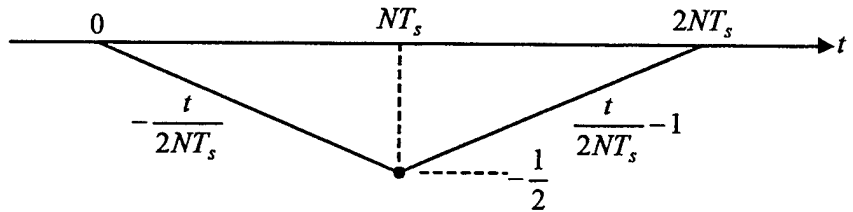
$k > N$



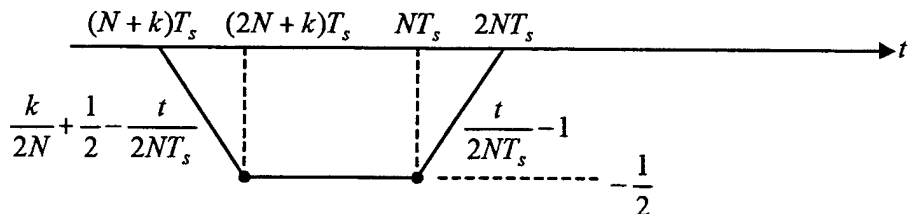
$-N < k < 0$



$k = -N$



$k < -N$



(note: not drawn to scale)

APPENDIX C: Determination of Significant Values of i (from Equation (19))**Case 1:** $0 < k \leq N$ For this set of k values,

$$p[t - 2iT, kT_s] = 0, \text{ for } 2iNT_s \geq 2NT_s \\ (0 \leq t \leq 2NT_s), (i \geq 1)$$

and

$$p[t - (2i + 1)T, kT_s] = 0, \text{ for } [(2i + 2)N + k]T_s \leq 0 \\ (0 \leq t \leq 2NT_s), (i \leq -2).$$

Thus, the set of significant $i = (0, -1)$.**Case 2:** $k > N$ For this set of k values,

$$p[t - 2iT, kT_s] = 0, \text{ for } 2iNT_s \geq 2NT_s \\ (0 \leq t \leq 2NT_s), (i \geq 1)$$

and

$$p[t - (2i + 1)T, kT_s] = 0, \text{ for } [(2i + 2)N + k]T_s \leq 0 \\ (0 \leq t \leq 2NT_s), \left(i \leq - \left[\frac{k}{2N} \right]_{int}^+ - 1 \right).$$

Thus, the set of significant $i = (0, -1, \dots, - \left[\frac{k}{2N} \right]_{int}^+)$.**Case 3:** $-N \leq k < 0$ For this set of k values,

$$p[t - 2iT, kT_s] = 0, \text{ for } (2iN + k)T_s \geq 2NT_s \\ (0 \leq t \leq 2NT_s), (i \geq 2)$$

and

$$p[t - (2i + 1)T, kT_s] = 0, \text{ for } (2i + 2)NT_s \leq 0 \\ (0 \leq t \leq 2NT_s), (i \leq -1).$$

Thus, the set of significant $i = (0, 1)$.**Case 4:** $k < -N$ For this set of k values,

$$p[t - 2iT, kT_s] = 0, \text{ for } (2iN + k)T_s \geq 2NT_s \\ (0 \leq t \leq 2NT_s), \left(i \geq \left[-\frac{k}{2N} \right]_{int}^+ + 1 \right)$$

and

$$p[t - (2i + 1)T, kT_s] = 0, \text{ for } (2i + 2)NT_s \leq 0 \\ (0 \leq t \leq 2NT_s), (i \leq -1).$$

Thus, the set of significant $i = (0, 1, \dots, \left[-\frac{k}{2N} \right]_{int}^+)$.

APPENDIX D: The Four Integrals of Equation (28)

Case 1: $0 \leq k_2 \leq k_1 - N - 1$

$$F_1(k_1, k_2) \equiv \frac{1}{2T} \int_0^{2T} \prod_{i=0}^{\left[\frac{k_1 - k_2}{2N} \right]_{int}^+} (\cdot) dt \quad (D1)$$

An exact evaluation of $F_1(k_1, k_2)$ seems to be unreasonably complicated to carry out. From the properties of $p[t, kT_s]$ (Appendix B), the following approximation is made.

$$p[t - 2iT, kT_s] \cong p[t - (2i + 1)T, kT_s] \cong -\frac{1}{2} \quad (\text{D2})$$

(for $0 \leq t \leq 2NT_s$).

Each factor in (\cdot) (see (29)) then becomes

$$\frac{1 \sin 4\pi h_0}{4 \sin \pi h_0} \cdot \frac{1 \sin 4\pi h_1}{4 \sin \pi h_1} = \cos \pi h_0 \cos \pi h_1 \cos 2\pi h_0 \cos 2\pi h_1. \quad (\text{D3})$$

The last step follows from (A6). $F_1(k_1, k_2)$ then becomes

$$F_1(k_1, k_2) \cong [\cos \pi h_0 \cos \pi h_1 \cos 2\pi h_0 \cos 2\pi h_1]^{1 + \left[\frac{k_1 - k_2}{2N} \right]_{int}^+}. \quad (\text{D4})$$

Case 2: $k_1 - N \leq k_2 \leq k_1 - 1$

$$F_2(k_1, k_2) \equiv \frac{1}{2T} \int_0^{2T} \prod_{i=0}^1 (\cdot) dt \quad (\text{D5})$$

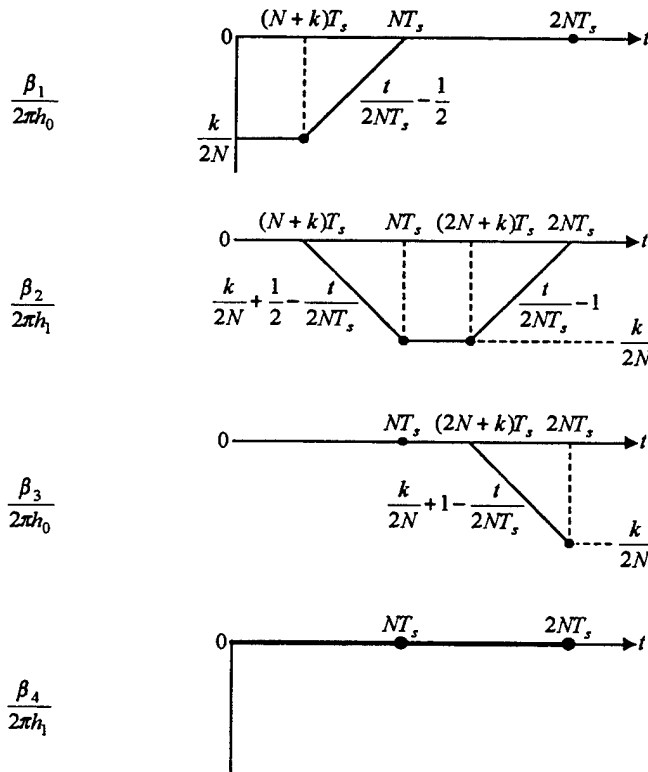
For this case, the integrand can be shown to be

$$\frac{1}{2} (\cos 3\beta_1 + \cos \beta_1) \cdot \frac{1}{2} (\cos 3\beta_2 + \cos \beta_2) + \frac{1}{2} (\cos 3\beta_3 + \cos \beta_3) \cdot \frac{1}{2} (\cos 3\beta_4 + \cos \beta_4),$$

using (A6), where

$$\begin{aligned} \beta_1 &= 2\pi h_0 p[t, kT_s] \\ \beta_2 &= 2\pi h_1 p[t - T, kT_s] \\ \beta_3 &= 2\pi h_0 p[t - 2T, kT_s] \\ \beta_4 &= 2\pi h_1 p[t - 3T, kT_s]. \end{aligned} \quad (\text{D6})$$

These are shown below, using Appendix B, for the range of the integral $(0, 2NT_s)$:



Thus, the integral becomes the sum of four parts:

$$\frac{1}{2NT_s} \left\{ \int_0^{(N+k)T_s} + \int_{(N+k)T_s}^{NT_s} + \int_{NT_s}^{(2N+k)T_s} + \int_{(2N+k)T_s}^{2NT_s} \right\}.$$

Evaluating these four and summing produces, after many tedious steps, the result is

$$\begin{aligned} F_2(k_1, k_2) = & \frac{1}{4} \left[1 + \frac{(k_2 - k_1)}{N} \right] \left[\cos \frac{3\pi h_0 (k_2 - k_1)}{N} + \cos \frac{\pi h_0 (k_2 - k_1)}{N} \right. \\ & \left. + \cos \frac{3\pi h_1 (k_2 - k_1)}{N} + \cos \frac{\pi h_1 (k_2 - k_1)}{N} \right] \\ & + \frac{1}{4\pi} \left\{ \left[\frac{h_1}{3(h_0^2 - h_1^2)} + \frac{3h_1}{h_0^2 - 9h_1^2} \right] \sin \frac{3\pi h_1 (k_2 - k_1)}{N} \right. \\ & + \left[\frac{h_1}{9h_0^2 - h_1^2} + \frac{h_1}{h_0^2 - h_1^2} \right] \sin \frac{\pi h_1 (k_2 - k_1)}{N} \\ & + \left[\frac{h_0}{9h_1^2 - h_0^2} + \frac{h_0}{h_1^2 - h_0^2} \right] \sin \frac{\pi h_0 (k_2 - k_1)}{N} \\ & \left. + \left[\frac{h_0}{3(h_1^2 - h_0^2)} + \frac{3h_0}{h_1^2 - 9h_0^2} \right] \sin \frac{3\pi h_0 (k_2 - k_1)}{N} \right\}. \end{aligned} \quad (D7)$$

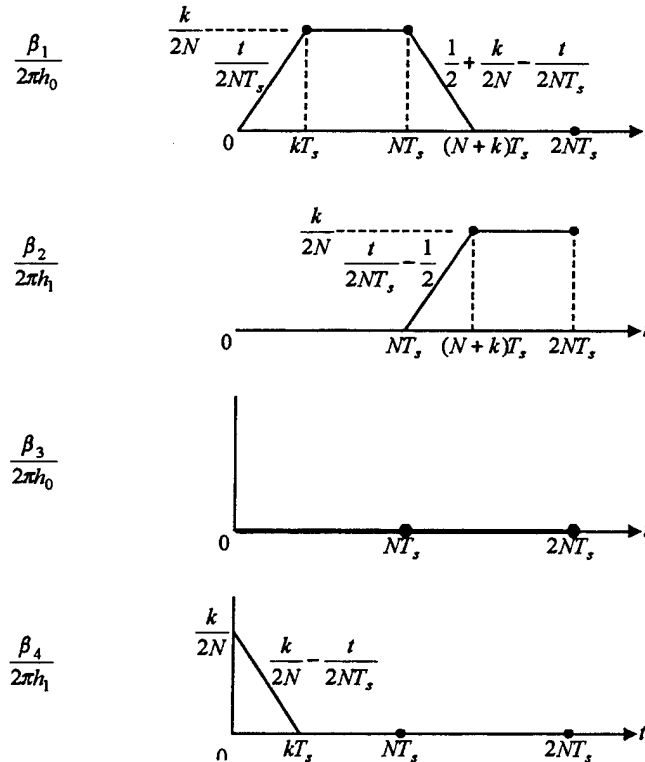
Case 3: $k_1 + 1 \leq k_2 \leq N + k_1$

$$F_3(k_1, k_2) \equiv \frac{1}{2T} \int_0^{2T} \prod_{i=-1}^0 (\cdot) dt \quad (D8)$$

We follow the same procedure used to obtain $F_2(k_1, k_2)$, except that now we need

$$\begin{aligned} \beta_1 &= 2\pi h_0 p[t, kT_s] \\ \beta_2 &= 2\pi h_1 p[t - T, kT_s] \\ \beta_3 &= 2\pi h_0 p[t + 2T, kT_s] \\ \beta_4 &= 2\pi h_1 p[t + T, kT_s]. \end{aligned} \quad (D9)$$

These are shown below for the range $(0, 2NT_s)$:



The integral becomes the sum of four parts,

$$\frac{1}{2NT_s} \left\{ \int_0^{kT_s} + \int_{kT_s}^{NT_s} + \int_{NT_s}^{(N+k)T_s} + \int_{(N+k)T_s}^{2NT_s} \right\},$$

requiring many tedious steps to produce the result:

$$\begin{aligned} F_3(k_1, k_2) = & \frac{1}{4} \left[1 - \frac{(k_2 - k_1)}{N} \right] \left[\cos \frac{3\pi h_0 (k_2 - k_1)}{N} + \cos \frac{\pi h_0 (k_2 - k_1)}{N} \right. \\ & \left. + \cos \frac{3\pi h_1 (k_2 - k_1)}{N} + \cos \frac{\pi h_1 (k_2 - k_1)}{N} \right] \\ & + \frac{1}{4\pi} \left\{ \left[\frac{h_1}{3(h_1^2 - h_0^2)} + \frac{3h_1}{9h_1^2 - h_0^2} \right] \sin \frac{3\pi h_1 (k_2 - k_1)}{N} \right. \\ & + \left[\frac{h_1}{h_1^2 - 9h_0^2} + \frac{h_1}{h_1^2 - h_0^2} \right] \sin \frac{\pi h_1 (k_2 - k_1)}{N} \\ & + \left[\frac{h_0}{h_0^2 - 9h_1^2} + \frac{h_0}{h_0^2 - h_1^2} \right] \sin \frac{\pi h_0 (k_2 - k_1)}{N} \\ & \left. + \left[\frac{h_0}{3(h_0^2 - h_1^2)} + \frac{3h_0}{9h_0^2 - h_1^2} \right] \sin \frac{3\pi h_0 (k_2 - k_1)}{N} \right\}. \end{aligned} \quad (D10)$$

Case 4: $N + k_1 + 1 \leq k_2 \leq NL_0 - 1$

$$F_4(k_1, k_2) \equiv \frac{1}{2T} \int_0^{2T} \prod_{i=-\left[\frac{k_2-k_1}{2N}\right]_{int}^+}^0 (\cdot) dt \quad (D11)$$

For this range of k_2 we make the approximations,

$$\begin{aligned} p[t - 2iT, kT_s] & \cong p[t - (2i + 1)T, kT_s] \cong \frac{1}{2} \\ & \text{(for } 0 \leq t \leq 2NT_s) \end{aligned} \quad (D12)$$

and follow the steps used in obtaining $F_1(k_1, k_2)$ to produce the result,

$$F_4(k_1, k_2) \cong [\cos \pi h_0 \cos \pi h_1 \cos 2\pi h_0 \cos 2\pi h_1]^{1+\left[\frac{k_2-k_1}{2N}\right]_{int}^+}. \quad (D13)$$

REPORT DOCUMENTATION PAGE

Form Approved
OMB No. 0704-0188

Public reporting burden for this collection of information is estimated to average 1 hour per response, including the time for reviewing instructions, searching existing data sources, gathering and maintaining the data needed, and completing and reviewing the collection of information. Send comments regarding this burden estimate or any other aspect of this collection of information, including suggestions for reducing this burden, to Washington Headquarters Services, Directorate for Information Operations and Reports, 1215 Jefferson Davis Highway, Suite 1204, Arlington, VA 22202-4302, and to the Office of Management and Budget, Paperwork Reduction Project (0704-0188), Washington, DC 20503.

1. AGENCY USE ONLY (Leave blank)		2. REPORT DATE <p style="text-align: center;">February 2000</p>	3. REPORT TYPE AND DATES COVERED <p style="text-align: center;">Final: Oct 1998 to Sept 1999</p>	
4. TITLE AND SUBTITLE A MAXIMUM-LIKELIHOOD-BASED FREQUENCY SYNCHRONIZER FOR DUAL-H FULL-RESPONSE 4-ARY CONTINUOUS-PHASE MODULATION (CPM)		5. FUNDING NUMBERS PE: 0601152N AN: DN307786 WU: ZU73		
6. AUTHOR(S) R. H. Pettit California State University, Northridge		B. E. Wahlen SSC San Diego		
7. PERFORMING ORGANIZATION NAME(S) AND ADDRESS(ES) SSC San Diego San Diego, CA 92152-5001		8. PERFORMING ORGANIZATION REPORT NUMBER TD 3094		
9. SPONSORING/MONITORING AGENCY NAME(S) AND ADDRESS(ES) Office of Naval Research 800 North Quincy Street Arlington, VA 22217-5660		10. SPONSORING/MONITORING AGENCY REPORT NUMBER		
11. SUPPLEMENTARY NOTES				
12a. DISTRIBUTION/AVAILABILITY STATEMENT Authorized for public release, distribution is unlimited.			12b. DISTRIBUTION CODE	
13. ABSTRACT (Maximum 200 words) <p>Maximum-likelihood techniques are useful in finding structures for synchronizers for various cases. Synchronizers for frequency, phase, and timing have been found for various bandpass signaling techniques such as PSK, DPSK, QAM, MSK, and CPM. These include data-aided, decision-directed, clock-aided cases. For Continuous-Phase Modulation (CPM), however, apparently only the single modulation index case has ML-based synchronizers.</p> <p>This report describes a new non-data-aided, non-decision-directed ML-based frequency synchronizer (with no phase or timing information) derived for a full-response, dual-h (two modulation indexes), 4-ary CPM signaling scheme. The derived structure will be incorporated into future simulations to compare performance among several possible frequency synchronizers.</p>				
14. SUBJECT TERMS Mission Area: Command, Control, and Communications continuous-phase modulation (CPM) frequency synchronization maximum-likelihood estimation dual-h CPM digital synchronizers			15. NUMBER OF PAGES <p style="text-align: center;">26</p>	
17. SECURITY CLASSIFICATION OF REPORT UNCLASSIFIED			16. PRICE CODE	
18. SECURITY CLASSIFICATION OF THIS PAGE UNCLASSIFIED		19. SECURITY CLASSIFICATION OF ABSTRACT UNCLASSIFIED		20. LIMITATION OF ABSTRACT SAME AS REPORT

21a. NAME OF RESPONSIBLE INDIVIDUAL

B. E. Wahlen

21b. TELEPHONE (include Area Code)

(619) 553-5622
e-mail: wahlen@spawar.navy.mil

21c. OFFICE SYMBOL

Code D841

INITIAL DISTRIBUTION

D0012	Patent Counsel	(1)
D0271	Archive/Stock	(6)
D0274	Library	(2)
D027	M. E. Cathcart	(1)
D0271	D. Richter	(1)
D841	B. E. Wahlen	(15)

Defense Technical Information Center
Fort Belvoir, VA 22060-6218 (4)

SSC San Diego Liaison Office
Arlington, VA 22202-4804

Center for Naval Analyses
Alexandria, VA 22302-0268

Navy Acquisition, Research and
Development Information Center
Arlington, VA 22202-3734

Government-Industry Data Exchange
Program Operations Center
Corona, CA 91718-8000

California State University, Northridge
Northridge, CA 91330-8346 (10)